DNA Repair Biomarker Profiling of Head and Neck Cancer: Ku80 Expression Predicts Locoregional Failure and Death following Radiotherapy

Benjamin J. Moeller[1], John S. Yordy[1], Michelle D. Williams[2], Uma Giri[1], Uma Raju[1], David P. Molkentine[1], Lauren A. Byers[3], John V. Heymach[3,4], Michael D. Story[5], J. Jack Lee[6], Erich M. Sturgis[7], Randal S. Weber[7], Adam S. Garden[1], K. Kian Ang[1], and David L. Schwartz[1]

Abstract

Purpose: Radiotherapy plays an integral role in the treatment of head and neck squamous cell carcinoma (HNSCC). Although proteins involved in DNA repair may predict HNSCC response to radiotherapy, none has been validated in this context. We examined whether differential expression of double-strand DNA break (DSB) repair proteins in HNSCC, the chief mediators of DNA repair following irradiation, predict for treatment outcomes.

Experimental Design: Archival HNSCC tumor specimens ($n = 89$) were assembled onto a tissue microarray and stained with antibodies raised against 38 biomarkers. The biomarker set was enriched for proteins involved in DSB repair, in addition to established mechanistic markers of radioresistance. Staining was correlated with treatment response and survival alongside established clinical and pathologic covariates. Results were validated in an independent intramural cohort ($n = 34$).

Results: Ku80, a key mediator of DSB repair, correlated most closely with clinical outcomes. Ku80 was overexpressed in half of all tumors, and its expression was independent of all other covariates examined. Ku80 overexpression was an independent predictor for both locoregional failure and mortality following radiotherapy ($P < 0.01$). The predictive power of Ku80 overexpression was confined largely to HPV-negative HNSCC, where it conferred a nine-fold greater risk of death at two years.

Conclusions: Ku80 overexpression is a common feature of HNSCC, and is a candidate DNA repair-related biomarker for radiation treatment failure and death, particularly in patients with high-risk HPV-negative disease. It is a promising, mechanistically rational biomarker to select individual HPV-negative HNSCC patients for strategies to intensify treatment. *Clin Cancer Res; 17(7); 2035–43. ©2011 AACR.*

Introduction

Radiotherapy, with or without concurrent chemotherapy, is the standard organ-preserving treatment of locally advanced HNSCC. As clinical outcomes have improved only modestly over the past several decades (1–3), treatment intensification is a focus of ongoing clinical trials. However, an inability to prospectively identify high-risk patients continues to make such efforts inefficient and exposes low-risk patients to unnecessary toxicity.

Current risk-stratification algorithms for HNSCC rely mostly on clinical data, such as AJCC stage and primary tumor subsite, which are only modestly predictive of outcomes (4, 5). Mechanistic biomarkers designed to refine prospective risk-stratification have not yet been integrated into clinical practice. The emergence of human papilloma virus (HPV)–associated HNSCC as a clinically and epidemiologically distinct disease may eventually lead to tailored therapy for this subset of head and neck cancers (6–8). However, more data are needed to better understand the biology of HPV-unassociated HNSCC, because patients with this disease continue to carry the highest risks of treatment failure.

Radiation therapy, like many cytotoxic chemotherapy agents, kills tumor cells by damaging DNA. Recent work has shown that the overexpression of proteins involved in DNA damage repair, such as ERCC1, has predictive and prognostic value for various tumor types treated with chemotherapy, particularly lung cancer treated by platinum agents (9, 10). Intuitively, DNA repair-related biomarkers would be particularly useful for predicting radiotherapy and chemoradiotherapy outcomes for HNSCC but none have yet been identified. Radiation causes many types of DNA damage, but the lesion contributing the most to target cell killing is the double-strand break (DSB; ref. 11). DSB

Authors' Affiliations: Departments of [1]Radiation Oncology, [2]Pathology, [3]Thoracic/Head and Neck Medical Oncology, [4]Cancer Biology, [6]Biostatistics, and [7]Head and Neck Surgery, University of Texas M.D. Anderson Cancer Center, Houston, Texas; and [5]Department of Radiation Oncology, University of Texas Southwestern Medical Center, Dallas, Texas

Note: Supplementary data for this article are available at Clinical Cancer Research Online (http://clincancerres.aacrjournals.org/).

J. S. Yordy and M. D. Williams contributed equally to this work.

Corresponding Author: David L. Schwartz, Department of Radiation Medicine, Hofstra North Shore-LIJ School of Medicine, 270-05 76th Avenue, New Hyde Park, NY 11040. Phone: 718-470-7190; Fax: 718-470-8445; E-mail: Dschwartz3@NSHS.edu

Translational Relevance

Roughly half of all head and neck cancer patients succumb to their diagnosis. Biomarkers identifying tumors at highest risk for failure are necessary to streamline clinical trial design by triaging patients toward appropriate treatment intensity. Although human papilloma virus (HPV) infection has emerged as an important prognostic marker of favorable outcome for head and neck cancers, specific markers are lacking to guide treatment of high-risk, HPV-unassociated tumors. We now demonstrate that patients with HPV-unassociated head and neck cancer expressing high levels of Ku80—a protein involved in repair of radiation-induced DNA damage—are at significantly higher risk for radiotherapy failure and death. This establishes Ku80 as the first candidate DNA repair biomarker to show potential predictive and prognostic value for head and neck radiotherapy.

repair involves a large network of proteins with complementary and redundant functions (12, 13). Therefore, proper understanding of DSB phenotypes in human tumor specimens, and their relationship to disease outcomes, will require broad profiling of involved proteins. In this report, we profile the expression of 18 major DSB repair factors, as well as proteins involved in complementary signaling pathways, in a cohort of archival HNSCC specimens of known HPV infection status from irradiated patients, and correlate these profiles with disease outcomes.

Materials and Methods

Patient materials

All patient specimens were obtained and handled in accordance with an Institutional Review Board approved protocol (LAB09-0215). A list of all HNSCC patients treated with intensity-modulated radiotherapy (IMRT) in the Department of Radiation Oncology at the University of Texas M. D. Anderson Cancer Center was cross-referenced with the institutional Head and Neck Tissue Bank. Patients with primary tumors outside the pharyngolaryngeal axis, those without pre-radiotherapy specimens in the Tissue Bank, and those receiving induction chemotherapy were excluded.

Paraffin blocks were retrieved for all remaining patients and evaluated for inclusion on a tissue microarray (TMA). In total, 89 patient specimens were included on a TMA, which constituted the testing set. For the validation set, 74 additional patient specimens were serially sectioned for analysis. Demographic, clinical, and treatment characteristics of cases in both the testing and validation sets were typical for head and neck radiotherapy patients at our institution: the patients were predominantly male smokers with stage IVa squamous cell carcinomas of the oropharynx, treated with radiotherapy alone (Table 1).

Local and systemic treatment

All patients were treated with IMRT, as described previously (14, 15). IMRT was delivered using step-and-shoot multileaf collimation through a static treatment gantry. Treatment planning was carried out on a Pinnacle³ system (version 6.2b or later, Philips Medical Systems). Surgery and chemotherapy were employed per standard institutional clinical practice (Table 1).

Biomarker analysis

Formalin-fixed paraffin-embedded specimens were processed and stained using standard immunohistochemical (IHC) methods. Specimens were cut at 4 μm thick, mounted onto positively charged slides, baked overnight, deparaffinized, then boiled in 10 mM citrate buffer (pH 6.0) for 20 minutes. Slides were blocked in 10% goat serum for 30 minutes at room temperature, incubated overnight with primary antibody at 4°, washed, incubated with secondary antibody for 30 minutes at room temperature, washed, developed using DAB+ reagent (Dako), counterstained with hematoxylin, dehydrated, and mounted under a coverslip (Supplementary Fig. S1). In total, 38 biomarkers were evaluated (manufacturer and dilution details listed in Supplementary Table 1).

Two physicians (BJM and MDW) independently scored intensity (0–3+) and percentage of staining (0%–100%) for each de-identified sample without knowledge of clinical data. Discrepancies between scores were rare, and were resolved by coordinated re-review of the slides between the scoring physicians. IHC scores were converted to nominal groupings (low, medium, high) according to a standardized algorithm (Supplementary Table S2).

Reverse phase protein array

A total of 28 HNSCC cell lines were acquired through the M.D. Anderson Cancer Center Head and Neck cell line repository or by the American Type Culture Collection. The identity of each cell line was confirmed by DNA fingerprinting via short tandem repeat (STR) profiling (PowerPlex 1.2, Promega). HPV-negativity was confirmed by PCR (not shown). Cells were starved of FBS for 24 hours, then stimulated with 10% fetal bovine serum 30 minutes prior to the collection of whole cell protein lysate (lysis buffer: 1% Triton X-100, 50 mM HEPES pH 7.4, 150 mM NaCl, 1.5 mM MgCl2, 1 mM EGTA, 100 mM NaF, 10 mM NaPPI, 10% glycerol, 1 mM phenylmethylsulfonyl fluoride, 1 mM Na3VO4, and 10 μg/mL aprotinin). Protein concentrations were normalized to 1 μg/μL, and denatured at 100°C for 5 minutes in 10% 2-mercaptoethanol, 8.75% glycerol, 2% SDS, and 0.625 M Tris-HCl (pH 6.8). Duplicate samples were then serially diluted (1:2–1:16), transferred to 384-well plates, and printed on nitrocellulose-coated glass FAST Slides (GE Whatman) using an Aushon 2470 Arrayer (Aushon Biosystems). The microarray slides were pre-cleared with reblot mild stripping solution (Millipore) for 5 minutes, then blocked for 30 minutes (I-block). Incubation with the anti-Ku80 primary antibody (Cell Signaling: 2180), secondary antibody, and secondary

Table 1. Demographic, clinical, and treatment characteristics for the two patient cohorts

		Testing set ($N = 89$)	Validation set ($N = 34$)
Age		60 (32–84)	59 (43–81)
Sex	Male	73 (82)	29 (85)
	Female	16 (18)	5 (15)
Tobacco	Yes	57 (64)	27 (79)
	No	32 (36)	7 (21)
HPV	Negative	53 (60)	34 (100)
	Positive	36 (40)	0 (0)
Overall stage	I	3 (3)	0 (0)
	II	12 (13)	4 (12)
	III	34 (38)	8 (24)
	IV	40 (46)	22 (64)
T stage	0	4 (4)	0 (0)
	1	27 (30)	11 (32)
	2	26 (30)	7 (21)
	3	15 (17)	10 (29)
	4	17 (19)	6 (18)
N stage	0	28 (31)	8 (24)
	1	8 (9)	2 (6)
	2	52 (59)	20 (58)
	3	1 (1)	4 (12)
Site	Oropharynx	61 (69)	23 (68)
	Larynx	21 (24)	10 (29)
	Hypopharynx	7 (7)	1 (3)
Radiation dose (Gy)		66 (60–70)	68 (60–72)
Radiation indication	Definitive	79 (89)	33 (97)
	Adjuvant	10 (11)	1 (3)
Chemotherapy	None	53 (60)	19 (56)
	Cisplatinum	36 (40)	15 (44)

NOTE. The number of cases or mean values for the group are provided, with percent of total or range of values in parentheses.

antibody amplification were carried out for 20, 20, and 15 minutes, respectively, with washing in TBST between each. Signal was detected using DAB chromogen for 5 minutes. Staining was captured using a CanoScan 8800 scanner with resolution set to 1200 DPI. RPPA data were quantified using SuperCurve methods (VigeneTech) and R (version 2.7.0).

Radiation clonogenic survival assay

Cells cultured under ambient growth conditions were exposed to a single fraction of ionizing radiation (2–6 Gy) using a Mark I 137Cs irradiator (325 cGy/min, J.L. Shepherd), allowed to grow for 10 to 14 days, fixed, stained, then scored for clonogenic survival. Surviving fractions were defined by the number of clonogens surviving to form colonies of at least 50 cells, normalized to the number of cells plated, and normalized to the plating efficiency for nonirradiated cells.

Statistical design and data analysis

We hypothesized that biomarkers could be found to discern an absolute survival advantage at 2 years following radiotherapy of 20% for patients with HNSCC. Based on a recent study of HPV-stratified HNSCC at the authors' institution (16), we anticipated finding a 2:1 ratio of patients with low-risk (i.e., HPV-positive) to high-risk (i.e., HPV-negative) tumors, with expected survival rates at 2 years of 95% ($\pm$2.3%) and 65% ($\pm$5.5%), respectively, and a combined overall 2 year mortality rate of 14% ($\pm$3.6%). To have 80% power to confirm our hypothesis with an α of 0.05, 89 patient samples were needed in the testing cohort.

Based on the findings from our testing cohort, our expected event rate was revised for the validation cohort. We anticipated that Ku80 overexpression would predict an absolute survival advantage at 2 years following radiotherapy of 50%. For an unselected patient population with an expected mortality rate of 14% ($\pm$3.6%), power calculations predicted that 74 samples would be needed to confirm a 20% absolute survival advantage (80% power, $\alpha = 0.05$); for a purely HPV-negative tumor cohort with an expected mortality rate of 45% ($\pm$4.8%), only 34 samples would be needed.

Patient demographic and clinicopathologic factors were collected, de-identified, and stored in a secured database alongside quantified immunohistochemical results. Survival rates were estimated using the Kaplan-Meier method. Comparisons between biomarker IHC staining groups (low, medium, high) were made using log-rank analysis with 2 degrees of freedom (SPSS version 16). Locoregional failure was defined as any persistence or recurrence of primary or regional nodal carcinoma following radiotherapy. Patients dying without evidence of locoregional failure were censored. The cumulative incidence rates of locoregional failure were calculated and compared using competing-risk methods, as previously described (17).

Frequency histograms of TMA staining scores were assembled, and comparisons between the HPV-positive and -negative groups were made using Student's t tests, with Bonferroni corrections applied for multiple comparisons (Microsoft Excel 2007). Correlations between and among clinical factors and biomarkers were calculated, with significant correlations defined as those with Spearman's rho coefficients greater than 0.5 (SPSS version 16). Univariate and multivariate analyses were performed based on Cox regression analyses (SPSS version 16), with IHC staining scores considered as ordinal single-level ordered variables. Unsupervised hierarchical clustering of TMA staining data was performed using average linkage clustering (Genesis version 1.7.5). Iterative processing was performed to search for the top n genes maximally discriminating survivors from nonsurvivors (Genesis version 1.7.5). Unless otherwise stated, significance was defined by a P value of less than 0.05.
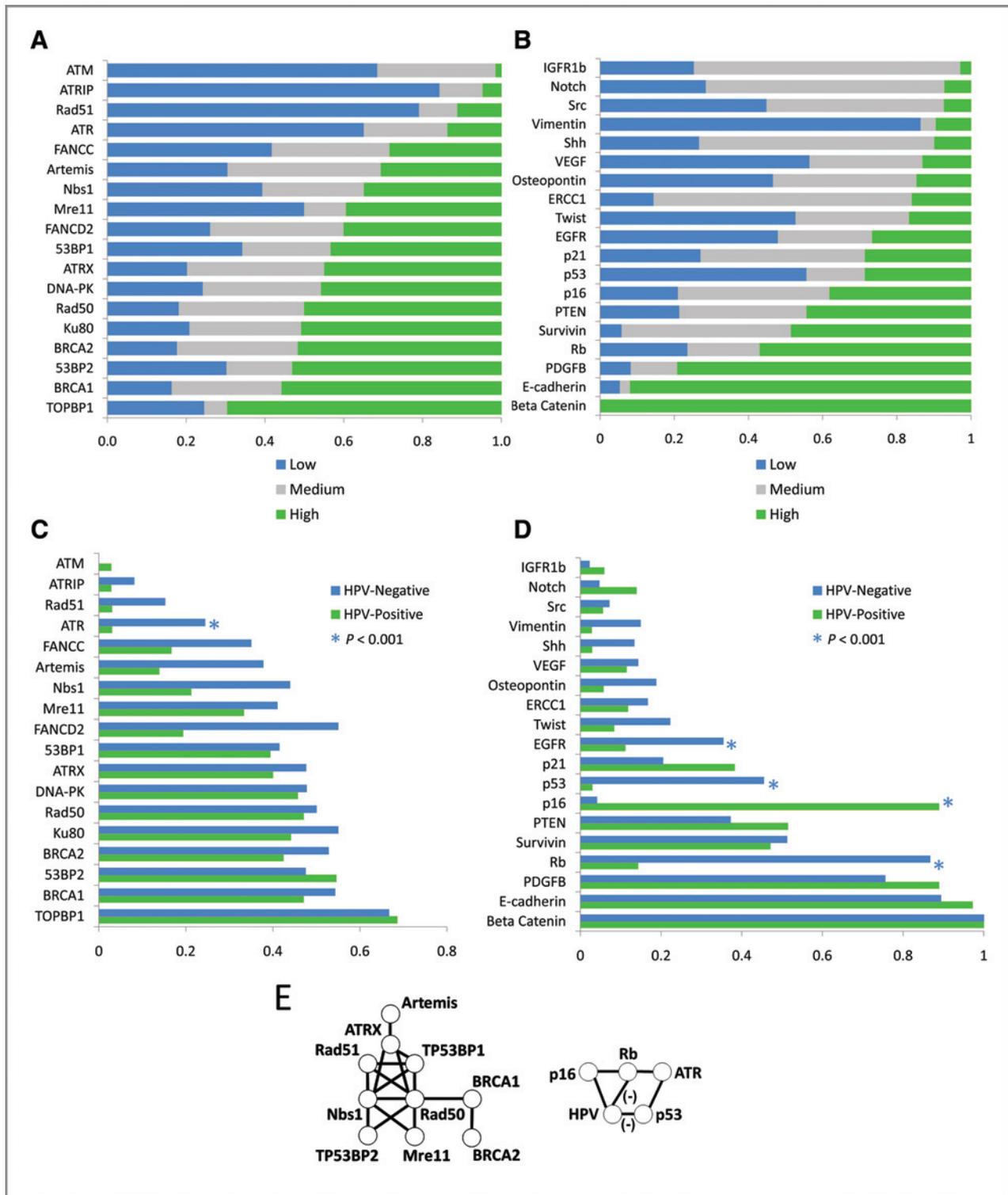
Figure 1. Biomarker profiles. A and B, histograms are shown displaying the fraction of samples expressing low (blue), medium (gray), or high (green) levels of each DSB-related (A) and DSB-unrelated (B) biomarker. Markers are listed in order of increasing overexpression. C and D, frequency histograms showing the likelihood of overexpression (i.e., IHC score = 3) for the displayed biomarkers, stratified by tumor HPV status. Both DSB-related (C) and DSB-unrelated (D) markers are shown. Patterns varying significantly by tumor HPV status are marked with an asterisk. (E) An interactivity map is shown, with lines connecting biomarkers with highly correlated expression patterns (Spearman's correlation coefficients ≥0.5). Two clusters are seen: an HPV cluster, and a homologous recombination cluster. All correlations are positive, except those between HPV and Rb, and HPV and p53(−).

Results

Radiotherapy outcome

At a median follow-up of 2 years, the locoregional control and overall survival rates for the testing cohort were 67.3% and 69.2%, respectively (Supplementary Fig. S2A and C). As expected, outcomes were significantly better for patients with HPV-positive tumors compared with those with HPV-negative tumors (Supplementary Fig. S2B and D).

Biomarker distribution

We first sought to descriptively characterize the expression profiles of the biomarkers examined on this study. Frequency histograms of expression scores are shown for the entire cohort, ranked in order of increasing rate of overexpression, for DSB biomarkers (Fig. 1A), and non-DSB biomarkers (Fig. 1B). None of the DSB biomarkers were universally overexpressed, but most of them were overexpressed in a majority of all cases. Interestingly, several major regulators of homologous recombination—including ATM, ATR, and Rad51—showed near-complete loss of expression in half to two thirds of all cases. Expression patterns of biomarkers unrelated to DNA damage repair indicate that the majority of tumors retained an epithelial phenotype (high E-cadherin and β-catenin, low Vimentin), with a relatively low level of expression of hypoxia markers (VEGF and Osteopontin). p53 was undetectable in approximately half of all samples, and p16 was overexpressed in approximately one third.

We confirmed HPV infection status of tumors in the testing set using a high-risk HPV genotype ISH probe set. We then stratified expression histograms by HPV status for both DSB- biomarkers (Fig. 1C) and DSB-unrelated biomarkers (Fig. 1D). Although there was a trend toward more frequent overexpression of homologous recombination proteins in HPV-negative tumors, ATR was the only factor significantly overrepresented in this cohort after correcting for multiple comparisons ($P < 0.001$). There were several significant differences in expression levels for DSB-unrelated biomarkers between HPV-positive and -negative tumors, all of which would be expected from the established biology of this virus (i.e., low p53, low pRb, high p16).

To better understand interactions occurring between the biomarkers studied, we next performed unsupervised hierarchical clustering of all derived expression profiles across the entire cohort (Supplementary Fig. S3). Proteins involved in DSB repair (nonhomologous end joining in red, homologous recombination in green) were tightly associated with one another, whereas biomarkers for other functional classifications were less well grouped. We also performed pairwise analyses to identify tight correlations between individual biomarkers, revealing a sizeable clustering of homologous recombination biomarkers, as well as a separate clustering of proteins affected by HPV (Fig. 1E).

Ku80 as an HNSCC biomarker

Iterative analyses of the hierarchically clustered profiles described earlier revealed no combination of biomarkers with significantly better predictive and prognostic value than individual biomarkers alone. Ku80 overexpression was most highly predictive of locoregional failure and death (not shown). We therefore abandoned clustering analysis in favor of linear modeling of risks of locoregional failure and death for each individual biomarker analyzed.

Table 2. Linear univariate and multivariate modeling of locoregional control (LRC) and overall survival (OS) probabilities as a function of clinical and biomarker covariates for the entire testing cohort

Endpoint	Biomarker	Spearman's rho coefficient	Univariate P value	Multivariate P value
LRC	Ku80	0.487	<0.005	0.007
	DNA-PKcs	0.305	0.006	NS
	p16	−0.224	0.04	NS
OS	Ku80	0.465	<0.005	<0.005
	T Stage	0.316	<0.005	NS
	HPV	−0.294	0.008	NS
	p16	−0.284	0.01	0.02
	DNA-PKcs	0.27	0.02	NS
	Shh	0.267	0.02	NS
	Rb	0.263	0.02	NS
	BRCA1	0.252	0.03	NS

NOTE. Positive correlations imply a larger risk of failure for increasing expression values or stage. NS, not significant ($P > 0.05$). All variables listed were included in both the univariate and multivariate analyses. Other variables included in the univariate analysis that were not predictive of outcomes are not listed here; these included N stage, overall stage, radiation dose, history of tobacco use, use of chemotherapy, primary tumor location, and the remainder of the biomarkers listed in Supplementary Table S1.

Univariate modeling identified overexpression of 2 non-homologous end-joining factors—Ku80 and DNA-PKcs—as predictive of locoregional failure (Table 2). Low p16 expression levels were also predictive of locoregional failure, as would be expected, although with lower correlation coefficients. On multivariate analysis, Ku80 was the only factor that remained predictive of locoregional treatment failure. Similar factors were also predictive of death on univariate analysis, but Ku80 and p16 remained the only markers predictive on multivariate analysis. With evidence supporting Ku80 as a predictor of both treatment failure and death, we next examined the influence of Ku80 expression levels on locoregional control and overall survival (Fig. 2). High levels of Ku80 expression were significantly predictive of both local failure and death ($P < 0.005$ for each).

Because low p16 expression, a marker for HPV-unassociated disease, was also predictive of death for these patients, we next sought to separately analyze the effect of biomarker expression levels on clinical outcomes after stratifying for HPV status. Ku80 retained its predictive power on multivariate analysis for both locoregional failure and death in the HPV-negative cohort (Supplementary Table S3), but lost this predictive power for the HPV-positive cohort (Supplementary Table S4). Accordingly, Ku80 overexpression predicted for a significantly higher risk of treatment failure and death for patients with HPV-negative disease ($P < 0.05$, Fig. 3A and B), but did not discriminate risk of treatment failure or death in patients with HPV-positive disease (not shown). Although there were several biomarkers predictive of treatment failure and death for patients with HPV-positive tumors by linear modeling (Supplementary Table S4), none of these ultimately predicted worse outcomes by cumulative incidence or Kaplan-Meier estimates (not shown), likely due to the low overall rate of clinical events in this patient subset.

We next sought to validate the above results in an independent cohort of patients. In light of the above results, the validation set ($n = 74$) was restricted to HPV-unassociated samples ($n = 34$), resulting in a cohort with baseline clinical and demographic characteristics similar to those of the testing population (Table 1). Locoregional control and overall survival rates for this cohort were qualitatively similar to those of the testing cohort (Fig. 3C and D), showing significantly worse outcomes for patients with tumors overexpressing Ku80 ($P < 0.01$).

Finally, we used reverse phase protein array technology to profile Ku80 expression levels across 28 HPV-negative HNSCC cell lines, and correlated these values with parameters of *in vitro* radiosensitivity. The fraction of cells surviving a single dose of 2 Gy (SF2, Fig. 4A) and 3.5 Gy (SF3.5, Fig. 4B) correlated directly with Ku80 expression levels. Corresponding to the clinical data described earlier, cell lines in the upper quartile of the Ku80 expression range were 6 times more likely to have radiation survival fractions above the mean than below.

Discussion

Preliminary results from prior studies have suggested an association between Ku protein expression and HNSCC radiation treatment outcome, but these existing data are limited by methodology and mixed findings (18–20). Our results provide strong evidence to suggest that Ku80 is a mechanistic determinant of tumor radioresistance and a biomarker for radiation treatment failure and death in patients with HPV-negative HNSCC. The ability to discriminate a 9-fold risk of death at 2 years suggests Ku80 to be a potentially valuable prognostic factor for this high-risk patient population, warranting consideration as a risk-stratification tool for future clinical trials of treatment intensification to enrich subpopulations of HPV-negative patients at highest risk for disease failure. Because Ku80 overexpression was a poor prognostic factor on this study irrespective of the use of concurrent chemotherapy, conventional platinum-based treatment intensification may
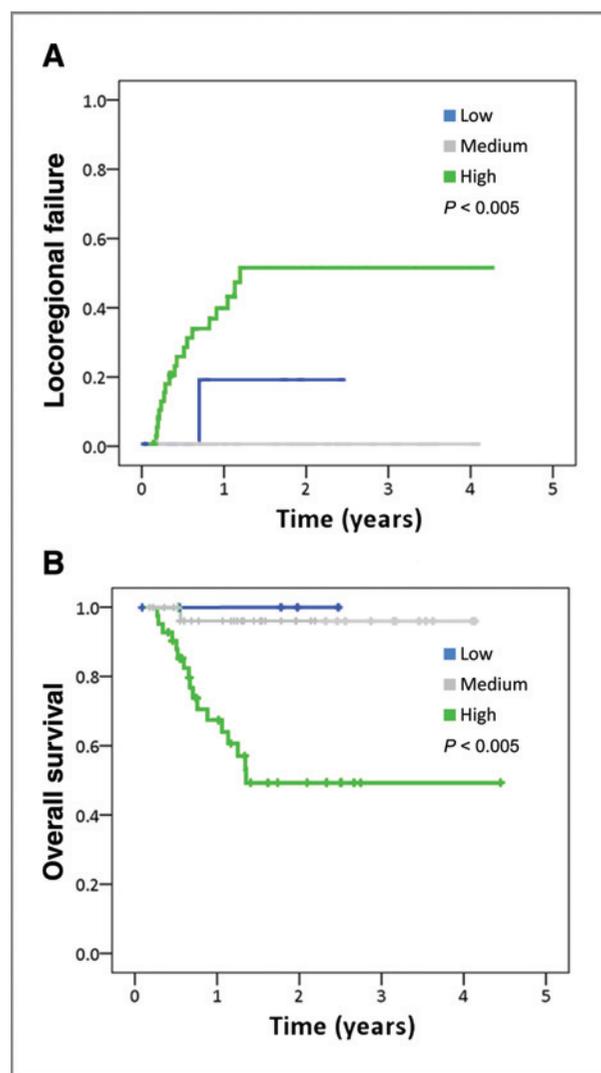

Figure 2. Cumulative locoregional failure (A) and overall survival (B) rates for the entire testing cohort as a function of Ku80 expression score.

Figure 3. Cumulative locoregional failure (A and C) and overall survival (B and D) rates for the HPV-negative subset of the testing cohort (A and B) and for the entire validation cohort (C and D) as a function of Ku80 expression score.
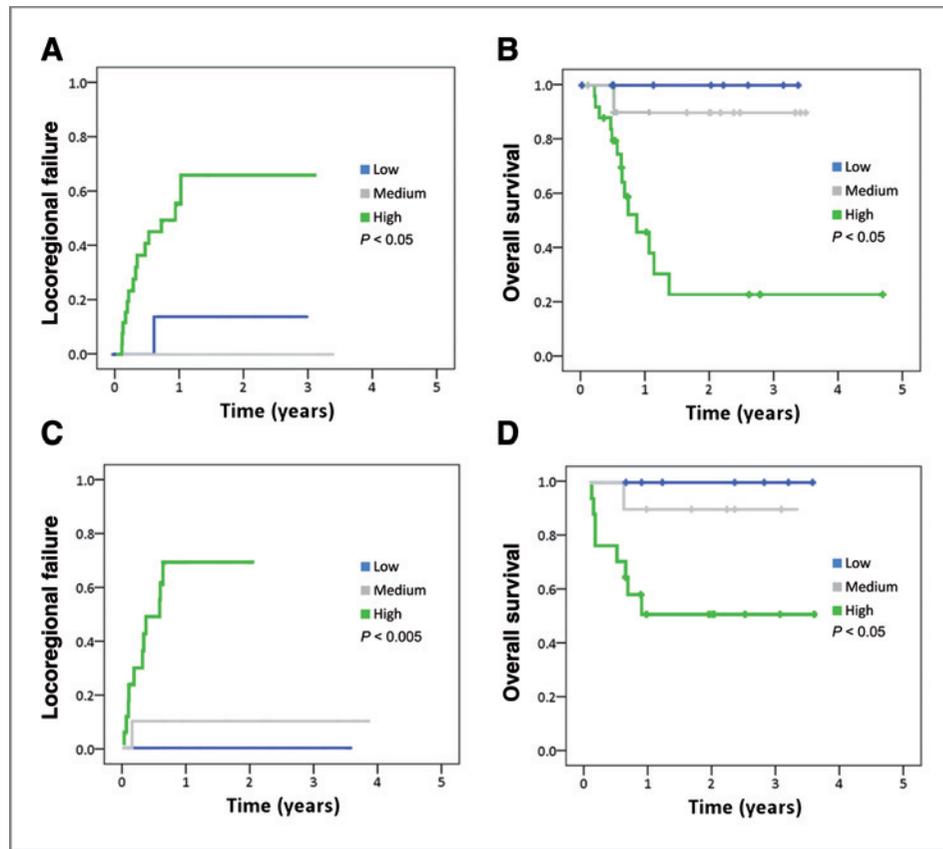
not be sufficient to overcome this mechanism of radio-resistance, and alternative strategies may be necessary.

There is mechanistic rationale to support an association between Ku80 expression and radioresistance. Ku80 is a key member of the nonhomologous end joining (NHEJ) pathway, the principal pathway used by healthy mammalian cells to repair DSBs (21). Its relative importance is likely greater for tumor cells, where defects in alternative pathways of DSB repair—including homologous recombination—establish a greater reliance on NHEJ (22). Ku80 participates in a heterodimeric complex which forms a hollow cylinder through which the open ends of DSBs are threaded, serving as a docking station for cofactors involved in downstream enzymatic break repair. Once docked onto a DSB, the Ku heterodimer recruits DNA-PKcs, which mediates secondary signaling events required

Figure 4. For 28 individual, HPV-negative HNSCC cell lines, relative Ku80 expression levels (by RPPA) are plotted against the fraction of cells surviving a single 2 Gy (A) and 3.5 Gy (B) dose of ionizing radiation. A solid line marks a linear regression through the data, showing a positive correlation between the variables. The horizontal dotted line marks the upper quartile of Ku80 expression values for the samples; the vertical dotted line marks the median SF2 and SF3.5 values. Marked in green are the cell lines falling within the upper quartile of Ku80 expression.
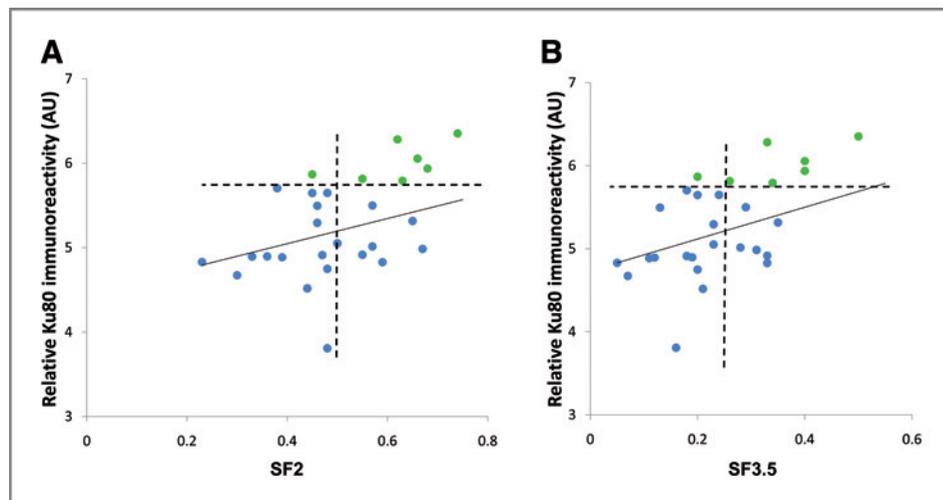
for repair (23). Experimental data directly link Ku80 with resistance to radiation (24, 25) and chemotherapy (26) in preclinical models.

In light of the fact that they are functionally related, it is interesting to note that Ku80 and DNA-PKcs expression patterns were not tightly correlated in our study (Spearman's coefficient <0.5), yet both predicted for local failure and death for patients with HPV-negative HNSCC. This may reflect parallel pathways impacting Ku80 and DNA-PKcs upregulation independently. This hypothesis warrants further investigation, and serves as a potential explanation for why clinically relevant DNA repair-related biomarkers have been slow to emerge to date. Interestingly, although Ku80 was predictive for outcomes of HPV-positive disease on univariate analysis, no DNA repair related protein had prognostic value for these patients by Kaplan-Meier analysis. Given the infrequency of events in this cohort, larger sampling will be required to definitively identify potential DNA repair-related biomarkers for HPV-associated HNSCC.

A number of additional observations from our results merit emphasis. First, in contrast to earlier reports (27–30), we found no association between mesenchymal or hypoxic phenotypes and treatment resistance when analyzed in the context of our broad biomarker panel. Although this may reflect limitations in patient and marker sampling, our data suggest relatively low activity in these pathways. Second, we saw no link between ERCC1 expression and treatment failure. Because chemotherapy was not the primary treatment modality used, and distant metastasis was an uncommon observation, this is not unexpected. Third, our findings establish a rationale for pursuing small molecule inhibitors of the NHEJ pathway for HPV-negative HNSCC. Moreover, the overall DSB protein profiles identified imply promising therapeutic opportunities beyond straightforward targeting of Ku80 and DNA-PKcs for radiosensitization. Attenuated expression of ATM and ATR in more than half of HNSCC tumors raises the possibility that such patients may be candidates for approaches which exploit synthetic lethality. Promotion of synthetic lethality through targeting of tumor DNA damage repair pathways has recently been validated by experimental and clinical demonstrations of efficacy of PARP inhibitors in BRCA-deficient tumors (31–33). Frequent loss of ATM and ATR may offer an opportunity to expand this paradigm into head and neck cancer.

There are limitations of this study which deserve mention. Because of practical limitations on tumor tissue procurement, patients in our study cohort constitute a minority of the overall HNSCC radiotherapy patient population at our institution, and secondary selection biases may have been introduced during this filtering process. In addition, although we studied as broad a selection of DSB-related proteins as possible, by necessity our panel represents an abridged list. Our knowledge of DSB repair is incomplete, and of factors known to be involved, some lack reproducible antibody-based detection. Although additional DNA repair biomarkers may remain unidentified by our analysis, our methodology provided robust protein-level data for Ku80 which could be validated both in cell lines and by additional patient sampling.

In summary, our findings establish Ku80 as a candidate DNA repair-related biomarker of radioresistance and treatment failure in HNSCC. It warrants follow-up validation as a risk-stratification tool for trials designed to individualize treatment intensification. Nonhomologous end joining proteins, including Ku80 and DNA-PKcs, are viable candidates for targeted inhibition for tumor radiosensitization of highest-risk HPV-negative cancer.

Disclosure of Potential Conflicts of Interest

No potential conflicts of interest were disclosed.

Grant Support

References

1. Denis F, Garaud P, Bardet E, Alfonsi M, Sire C, Germain T, et al. Final results of the 94–01 French Head and Neck Oncology and Radiotherapy Group randomized trial comparing radiotherapy alone with concomitant radiochemotherapy in advanced-stage oropharynx carcinoma. J Clin Oncol 2004;22:69–76.
2. Bonner JA, Harari PM, Giralt J, Azarnia N, Shin DM, Cohen RB, et al. Radiotherapy plus cetuximab for squamous-cell carcinoma of the head and neck. N Engl J Med 2006;354:567–78.
3. Jeremic B, Shibamoto Y, Milicic B, Nikolic N, Dagovic A, Aleksandrovic J, et al. Hyperfractionated radiation therapy with or without concurrent low-dose daily cisplatin in locally advanced squamous cell carcinoma of the head and neck: a prospective randomized trial. J Clin Oncol 2000;18:1458–64.
4. Cooper JS, Farnan NC, Asbell SO, Rotman M, Marcial V, Fu KK, et al. Recursive partitioning analysis of 2105 patients treated in Radiation Therapy Oncology Group studies of head and neck cancer. Cancer 1996;77:1905–11.
5. Leon X, Gich I, Orus C, Del Prado Venegas M, Ramon Gras J, Quer M. Comparison of the Radiation Therapy Oncology Group recursive partitioning classification and Union Internationale Contre le Cancer TNM classification for patients with head and neck carcinoma. Head Neck 2005;27:248–57.
6. Gillison ML, D'Souza G, Westra W, Sugar E, Xiao W, Begum S, et al. Distinct risk factor profiles for human papillomavirus type 16-positive and human papillomavirus type 16-negative head and neck cancers. J Natl Cancer Inst 2008;100:407–20.
7. Kumar B, Cordell KG, Lee JS, Worden FP, Prince ME, Tran HH, et al. EGFR, p16, HPV titer, Bcl-xL and p53, sex, and smoking as indicators of response to therapy and survival in oropharyngeal cancer. J Clin Oncol 2008;26:3128–37.

8. Ang KK, Harris J, Wheeler R, Weber R, Rosenthal DI, Nguyen-Tân PF, et al. Human Papillomavirus and survival of patients with oropharyngeal cancer. N Engl J Med 2010;363:24–35.

9. Olaussen KA, Dunant A, Fouret P, Brambilla E, André F, Haddad V, et al. DNA repair by ERCC1 in non-small-cell lung cancer and cisplatin-based adjuvant chemotherapy. N Engl J Med 2006;355:983–91.

10. Handra-Luca A, Hernandez J, Mountzios G, Taranchon E, Lacau-St-Guily J, Soria JC, et al. Excision repair cross complementation group 1 immunohistochemical expression predicts objective response and cancer-specific survival in patients treated by Cisplatin-based induction chemotherapy for locally advanced head and neck squamous cell carcinoma. Clin Cancer Res 2007;13:3855–9.

11. Hall E, Giaccia A. Radiobiology for the Radiologist. 6th ed. Philadelphia: Lippincott Williams & Wilkins; 2006.

12. Matsuoka S, Ballif BA, Smogorzewska A, McDonald ER 3rd, Hurov KE, Luo J, et al. ATM and ATR substrate analysis reveals extensive protein networks responsive to DNA damage. Science 2007;316:1160–6.

13. Pan X, Ye P, Yuan DS, Wang X, Bader JS, Boeke JD. A DNA integrity network in the yeast Saccharomyces cerevisiae. Cell 2006;124:1069–81.

14. Dabaja B, Salehpour MR, Rosen I, Tung S, Morrison WH, Ang KK, et al. Intensity-modulated radiation therapy (IMRT) of cancers of the head and neck: comparison of split-field and whole-field techniques. Int J Radiat Oncol Biol Phys 2005;63:1000–5.

15. Garden AS, Morrison WH, Wong PF, Tung SS, Rosenthal DI, Dong L, et al. Disease-control rates following intensity-modulated radiation therapy for small primary oropharyngeal carcinoma. Int J Radiat Oncol Biol Phys 2007;67:438–44.

16. Moeller BJ, Rana V, Cannon BA, Williams MD, Sturgis EM, Ginsberg LE, et al. Prospective imaging assessment of mortality risk after head-and-neck radiotherapy. Int J Radiat Oncol Biol Phys 2010;78:667–74.

17. Pepe MS, Mori M. Kaplan-Meier, marginal or conditional probability curves in summarizing competing risks failure time data?Stat Med 1993;12:737–51.

18. Friesland S, Kanter-Lewensohn L, Tell R, Munck-Wikland E, Lewensohn R, Nilsson A. Expression of Ku86 confers favorable outcome of tonsillar carcinoma treated with radiotherapy. Head Neck 2003;25:313–21.

19. Lee SW, Cho KJ, Park JH, Kim SY, Nam SY, Lee BJ, et al. Expressions of Ku70 and DNA-PKcs as prognostic indicators of local control in nasopharyngeal carcinoma. Int J Radiat Oncol, Biol, Phys 2005;62:1451–7.

20. Pavón MA, Parreño M, León X, Sancho FJ, Céspedes MV, Casanova I, et al. Ku70 predicts response and primary tumor recurrence after therapy in locally advanced head and neck cancer. Int J Cancer 2008;123:1068–79.

21. Mahaney BL, Meek K, Lees-Miller SP. Repair of ionizing radiation-induced DNA double-strand breaks by non-homologous end-joining. Biochem J 2009;417:639–50.

22. Powell SN, Kachnic LA. Therapeutic exploitation of tumor cell defects in homologous recombination. Anticancer Agents Med Chem 2008;8:448–60.

23. Collis SJ, DeWeese TL, Jeggo PA, Parker AR. The life and death of DNA-PK. Oncogene 2005;24:949–61.

24. Chang HW, Kim SY, Yi SL, Son SH, Song do Y, Moon SY, et al. Expression of Ku80 correlates with sensitivities to radiation in cancer cell lines of the head and neck. Oral Oncol 2006;42:979–86.

25. Nimura Y, Kawata T, Uzawa K, Okamura J, Liu C, Saito M, et al. Silencing Ku80 using small interfering RNA enhanced radiation sensitivity in vitro and in vivo. Int J Oncol 2007;30:1477–84.

26. Kim SH, Kim D, Han JS, Jeong CS, Chung BS, Kang CD, et al. Ku autoantigen affects the susceptibility to anticancer drugs. Cancer Res 1999;59:4012–7.

27. Silva P, Slevin NJ, Sloan P, Valentine H, Cresswell J, Ryder D, et al. Prognostic significance of tumor hypoxia inducible factor-1alpha expression for outcome after radiotherapy in oropharyngeal cancer. Int J Radiat Oncol, Biol, Phys 2008;72:1551–9.

28. Le QT, Kong C, Lavori PW, O'byrne K, Erler JT, Huang X, et al. Expression and prognostic significance of a panel of tissue hypoxia markers in head-and-neck squamous cell carcinomas. Int J Radiat Oncol, Biol, Phys 2007;69:167–75.

29. Chung CH, Parker JS, Karaca G, Wu J, Funkhouser WK, Moore D, et al. Molecular classification of head and neck squamous cell carcinomas using patterns of gene expression. Cancer Cell 2004;5:489–500.

30. Chung CH, Parker JS, Ely K, Carter J, Yi Y, Murphy BA, et al. Gene expression profiles identify epithelial-to-mesenchymal transition and activation of nuclear factor-kappaB signaling as characteristics of a high-risk head and neck squamous cell carcinoma. Cancer Res 2006;66:8210–8.

31. Farmer H, McCabe N, Lord CJ, Tutt AN, Johnson DA, Richardson TB, et al. Targeting the DNA repair defect in BRCA mutant cells as a therapeutic strategy. Nature 2005;434:917–21.

32. Bryant HE, Schultz N, Thomas HD, Parker KM, Flower D, Lopez E, et al. Specific killing of BRCA2-deficient tumours with inhibitors of poly(ADP-ribose) polymerase. Nature 2005;434:913–7.

33. Fong PC, Boss DS, Yap TA, Tutt A, Wu P, Mergui-Roelvink M, et al. Inhibition of poly(ADP-ribose) polymerase in tumors from BRCA mutation carriers. N Engl J Med 2009;361:123–34.